Journal of Power Sources 273 (2015) 237–243

Contents lists available at ScienceDirect

Journal of Power Sources

journal homepage: www.elsevier.com/locate/jpowsour

High temperature mechanical properties of zirconia tapes used for electrolyte supported solid oxide fuel cells

Felix Fleischhauer [a, b, *], Raul Bermejo [b], Robert Danzer [b], Andreas Mai [c], Thomas Graule [a], Jakob Kuebler [a]

[a] Empa, Swiss Federal Laboratories for Materials Science and Technology, Laboratory for High Performance Ceramics, Ueberlandstr. 129, 8600 Duebendorf, Switzerland
[b] Institut für Struktur- und Funktionskeramik, Montanuniversität Leoben, Peter-Tunner-Str. 5, 8700 Leoben, Austria
[c] Hexis Ltd., Zum Park 5, 8404 Winterthur, Switzerland

HIGHLIGHTS

- The elastic constants of 6ScSZ and 6Sc1CeSZ were measured from RT up 950 °C.
- We determined the fracture toughness of four zirconia compounds from RT-850 °C.
- Sub critical crack growth parameters were determined at elevated temperatures.
- We found that the fracture toughness can be obtained from strength measurements.
- At $T = 850$ °C the cubic 10Sc1CeSZ can be as reliable as the tetragonal 3YSZ and 6ScSZ.

ARTICLE INFO

Article history:
Received 16 July 2014
Received in revised form
3 September 2014
Accepted 9 September 2014
Available online 19 September 2014

Keywords:
Scandia stabilized zirconia
Strength
Sub critical crack growth
Reliability
Elastic constants

ABSTRACT

Solid-Oxide-Fuel-Cell systems are efficient devices to convert the chemical energy stored in fuels into electricity. The functionality of the cell is related to the structural integrity of the ceramic electrolyte, since its failure can lead to drastic performance losses. The mechanical property which is of most interest is the strength distribution at all relevant temperatures and how it is affected with time due to the environment.

This study investigates the impact of the temperature on the strength and the fracture toughness of different zirconia electrolytes as well as the change of the elastic constants. 3YSZ and 6ScSZ materials are characterised regarding the influence of sub critical crack growth (SCCG) as one of the main lifetime limiting effects for ceramics at elevated temperatures. In addition, the reliability of different zirconia tapes is assessed with respect to temperature and SCCG. It was found that the strength is only influenced by temperature through the change in fracture toughness. SCCG has a large influence on the strength and the lifetime for intermediate temperature, while its impact becomes limited at temperatures higher than 650 °C. In this context the tetragonal 3YSZ and 6ScSZ behave quite different than the cubic 10Sc1CeSZ, so that at 850 °C it can be regarded as competitive compared to the tetragonal compounds.

© 2014 Elsevier B.V. All rights reserved.

1. Introduction

Electrolyte supported solid oxide fuel cells (SOFCs) are state of the art electro-chemical devices, which are employed for the efficient conversion of chemical energy stored within a fuel (e.g. natural or bio gas) into electricity. Such systems contain many ceramic components, which have to maintain their structural integrity in order to function properly throughout the whole targeted lifetime. Here the electrolyte is responsible for the cells structural integrity, while physically separating the fuel and the air from one another

* Corresponding author. Empa, Swiss Federal Laboratories for Materials Science and Technology, Laboratory for High Performance Ceramics, Ueberlandstr. 129, 8600 Duebendorf, Switzerland.
E-mail addresses: Felix.Fleischhauer@empa.ch (F. Fleischhauer), raul.bermejo@unileoben.ac.at (R. Bermejo), isfk@unileoben.ac.at (R. Danzer), Andreas.Mai@hexis.com (A. Mai), Thomas.Graule@empa.ch (T. Graule), Jakob.Kuebler@empa.ch (J. Kuebler).

http://dx.doi.org/10.1016/j.jpowsour.2014.09.068
0378-7753/© 2014 Elsevier B.V. All rights reserved.

and providing a sufficient ionic conductivity. If the separation is not maintained, intra cellular leakage will negatively affect the cell and stack performance instantaneously, which is the case, if the electrolyte fractures.

In order to predict the risk of failure a prospective electrolyte has to be properly characterized regarding its mechanical behaviour within a system specific environment, which is characterised by mechanical stresses, temperature and the presence of chemically active species. Since the state of the art electrolytes are brittle ceramics, such as zirconia and ceria-gadolinia, the strength depends in principle on two material specific features: the flaw size and shape distribution, within the components volume or at the surface, and its fracture toughness [1]. Both are first of all influenced by the material selection, processing and handling but also later on by the exposure to a system specific environment, where mechanical stresses, elevated temperatures and the contact with other components may alter these properties either instantaneously or with time. For instance sub critical crack growth (SCCG) [2–5] and cracks growing from the electrodes into the electrolyte [6,7] in combination with an applied stress influence the flaw size distribution whereas temperature itself changes the toughness. Ageing effects which are diffusion controlled and thus time dependent processes may also decrease or increase the materials resistance towards fracture [8–10] or change the stress state due to creep relaxation. All these aspects have to be considered, when assessing the reliability of a ceramic component, while the proper and accurate determination of the initial strength distribution, which reflects the initial flaw size distribution, is the most crucial one. A comprehensive overview of the available strength data of commercial and experimental yttria stabilized zirconia and ceria–gadolinia tapes was given by Nakajo et al. [11], while scandia stabilized zirconia has received less attention [12–14]. Studies investigating the specific reliability of anode supported SOFCs for a given load environment were already undertaken by Nakajo et al. and Clague et al. [15,16]. However they lack a sound knowledge of the aforementioned material specific behaviour, simply due to the huge effort, which is required to thoroughly gather all necessary parameters.

Hence this study aims to provide understanding on how the temperature influences the mechanical properties such as strength, fracture toughness, sub critical crack growth and the elastic constants of zirconia-based SOFC electrolytes. The emphasis here lies on the characterization of scandia doped zirconia electrolytes, which are known for their high ionic conductivity [17] and 3 mol% yttria stabilized zirconia (3YSZ) as a reference material. The reliability of these tapes is discussed considering thermal stresses and clamping loads and the evolution of their strength at elevated temperatures taking sub critical crack growth and the change of the elastic constants into account.

2. Experimental

The experimental investigation is centred on four different zirconia compounds. The tape samples of 6ScSZ (commercial code: FF-2003501), 6Sc1CeSZ (FF-2003507), 10Sc1CeSZ (FF-2003505) and 3YSZ (FF-2003504) were supplied by Hexis (Winterthur, Switzerland) and had a nominal thickness of 160, 110, 230 and 140 μm respectively.

The elastic constants of 3YSZ, 6ScSZ, 6Sc1CeSZ were measured at various temperatures using the Impulse-Excitation-Technique (IET) as described in Ref. [18], while bearing the rectangular plates (12 × 45 × 3.25 mm) either on a cross or two parallel bars in order to measure either their flexural or torsional frequencies in accordance with the EN 843-2 standard. These frequencies are then converted into the Young's and shear modulus following the approach of Spinner and Tefft [19]. The samples were manufactured

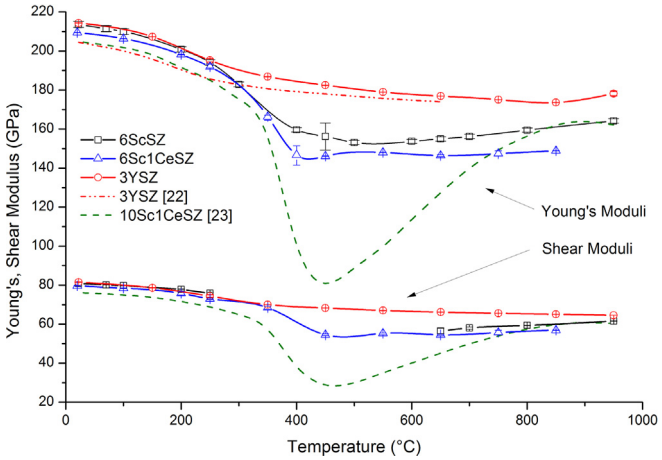

Fig. 1. Young's and shear modulus at varying temperatures for 3YSZ, 6ScSZ and 6Sc1CeSZ including the standard deviation of each measurement. A reference curve is taken for 3YSZ from Ref. [22], while the values of 10Sc1CeSZ are taken from Ref. [23].

via uniaxial pressing and sintering from the same powder (also supplied from Hexis) as was used for the respective tapes, except for 3YSZ, which was purchased from Tosoh (Tokyo, Japan). The powders have an average grain size between 0.5 and 0.6 μm and were sintered at 1580 °C for 2 h. The sample densities were determined via the dimensions and the weight and are greater than 98% of the theoretical density.

Ball-on-3-Balls (B3B) tests were conducted on rectangular specimens as described in Ref. [20]. For 3YSZ, 6ScSZ, 10Sc1CeSZ the rougher tape side (side which was cast onto the support foil) and for 6Sc1CeSZ the dull appearing side (side which was opposite to the support foil during the casting process) was consequently tested. If otherwise, it is explicitly mentioned. The strength analysis of these bending tests is based on the work of Börger et al. [21], where the maximum principle stress σ_{max} is related to the fracture force F by:

$$\sigma_{max} = f\frac{F}{t^2} \tag{1}$$

where t is the specimen thickness and f is a dimensionless proportionality factor, which depends on the thickness, size and Poisson's ratio of the specimen and the diameter of the balls. This factor and the corresponding effective surface area have been calculated for balls with a diameter of 2.2 mm and plates of $4 \times 3\ mm^2$ using the same finite element-model as in Ref. [20], with the same test rig as described in Ref. [13]. The results are comprised in following sample and test rig specific fit-function:

$$f = 0.214 + \frac{(2.914 + 9.96\,mm^{-1}\,t - 4.65\,mm^{-2}\,t^2)\,(1 + 0.939\nu)}{1 + 9.63\,mm^{-1}\,t} \tag{2}$$

which for thicknesses between $0.1 \le t \le 0.4$ mm and a Poisson's ratio between $0.2 \le \nu \le 0.4$ expresses f with an error of less than 1%:

All B3B-tests have been performed in a force controlled mode providing a constant force rate (N s^{-1}) during each test. Using Equations (1) and (2) the applied load rate (MPa s^{-1}) can be obtained, which was between 700 and 1000 MPa s^{-1} (so that fracture occurred in less than 2 s), if not mentioned otherwise.

3. Results

3.1. Elastic constants as a function of temperature

In order to describe the elastic behaviour of thin plates the Young's modulus and the Poisson's ratio have to be known and since electrolytes are operated at elevated temperatures, their elastic constants also have to be known at these conditions. Fig. 1 shows the results of the IET experiments. Additionally the Young's modulus of 3YSZ is plotted according to Giraud and Canel [22], which was measured using the same technique. Furthermore, the elastic constants of 10Sc1CeSZ are shown, which were taken from Kushi et al. [23] and which will be used for the following discussion of the present 10Sc1CeSZ tapes.

All zirconia compounds display the same behaviour, while possessing comparable Young's and shear moduli up to a temperature of 250 °C. While 3YSZ then continues its monotonic decay agreeing with the data given in Ref. [22], all other compounds run through a minimum between 400 and 500 °C, which becomes more pronounced as the content of doping is increased. This minimum is accompanied by increased internal friction and damping [23]. This damping is responsible that the shear modulus of 6ScSZ cannot be obtained by the applied method over a large temperature range between 300 °C and 600 °C. This is, because any torsional excitement is quickly absorbed, therefore no torsional vibration of the sample can be detected. The values taken for further discussion and analysis of the four different materials investigated in the present study are given in Table 1, including the standard deviation of the three samples from this study, which was calculated from at least ten single experiments per sample and temperature.

3.2. High temperature inert strength

The operating temperature of electrolyte supported SOFCs is typically between 700 °C and 900 °C, while the trend goes to ever decreasing temperatures. Therefore the strength of an electrolyte has to be known over the temperature range from room temperature to operating temperatures, in order to assess its suitability from a reliability point of view. For this purpose the four different zirconia compounds were investigated regarding their material specific temperature dependent strength. Since this behaviour does typically not depend on the size of flaws, the B3B-test was adapted for high temperature measurements by applying a test rig manufactured from alumina. For every temperature step at least 10 specimens per material were tested, selecting for 6ScSZ, 10Sc1CeSZ and 3YSZ the rough sides of the tapes and for 6Sc1CeSZ the dull sides. To avoid SCCG all tests were conducted in dry argon (80%)/oxygen (20%). The oxygen was to ensure that zirconia does not get reduced at the surface, since it is unknown how this would affect the strength or the toughness.

Table 2 shows the results of the median strength for different temperature levels. For all materials 30 specimens were tested at RT, which resulted in a Weibull modulus for 3YSZ, 6ScSZ, 6Sc1CeSZ and 10Sc1CeSZ of $m_{3YSZ,RT} = 20$, $m_{6ScSZ,RT} = 18$, $m_{6Sc1CeSZ,RT} = 20$ and $m_{10Sc1CeSZ,RT} = 11$, respectively. For 6ScSZ and 3YSZ the Weibull modulus at RT was reproduced at 850 °C testing more than 20 specimens ($m_{3YSZ,850\,°C} = 20$, $m_{6ScSZ,850\,°C} = 18$), which supports the assumption, that also at elevated temperatures the distribution and thus failure mechanism does not change and the same flaws are governing fracture. According to the Griffith criterion:

$$K_{Ic} = \sigma_{frac} Y \sqrt{\pi a} \tag{3}$$

the fracture toughness K_{Ic} is proportional to the fracture stress σ_{frac}. Therefore, the change in strength is solely attributed to a change in fracture toughness, making it possible to apply the following relation as a consequence of Equation (3) between the strength and the toughness:

$$\frac{\sigma(T_1)}{\sigma(T_2)} = \frac{K_{Ic}(T_1)}{K_{Ic}(T_2)} \tag{4}$$

so that the temperature dependency of the toughness can be obtained (see also Table 2), applying the RT toughness values given in Ref. [13]. Fig. 2 shows the toughness normalised to the RT-values. The applicability of Equation (4) is not always given, since flaws may alter with temperature. Comparing however the dull and the rough side of 6ScSZ and taking the directly measured toughness of 3YSZ into account, shows that for zirconia and the considered temperature range Equation (4) holds and delivers values within a justifiable error.

It is remarkable that the zirconia compounds consisting predominately of the tetragonal phase behave fairly the same, following the same monotonic decay, which is probably governed by the ability of the tetragonal phase to transform into the monoclinic phase and leads to the well-known transformation toughening [25]. The higher the temperature the lower the driving force for this transformation and hence the volume fraction at a crack tip, which transforms, decreases lowering the toughening effect. 10Sc1CeSZ does not possess this mechanism, which is why it has the lowest toughness to begin with. Its toughness is mainly determined by the surface energy, which together with the fracture toughness is proportional to the Young's modulus [26]. Hence, 10Sc1CeSZ follows qualitatively the trend of its Young's modulus shown in Fig. 1, which is in agreement with the strength data, toughness and Young's modulus published by Orlovskaya et al. [18] and has also been found for cubic 8YSZ [2].

For SOFCs the dominant mechanical loads are typically deformation controlled, which means that a material has rather to sustain a certain deformation rather than a force or stress. This happens for thermal stresses, residual stresses within the cell due

Table 1
Elastic parameters used for further discussion including the standard deviation given in the brackets. The Poisson's ratio ν was calculated from the shear (G) and the Young's modulus (E) according to $\nu = E/2G - 1$.Values of 10Sc1CeSZ are taken from Ref. [23].

Temperature (°C)	3YSZ		6ScSZ		6Sc1CeSZ		10Sc1CeSZ	
	E (GPa)	ν	E (GPa)	ν	E (GPa)	ν	E (GPa)	ν
25	214.3 (±0.1)	0.314 (±0.002)	213.6 (±1.5)	0.321 (±0.005)	209.5 (±0.1)	0.314 (±0.001)	204.6	0.345
250	195.2 (±0.8)	0.312 (±0.002)	194.2 (±1.4)	0.280 (±0.01)	191.9 (±1.4)	0.314 (±0.004)	185.0	0.345
350	–	–	–	–	–	–	155.7	0.361
450	182.5 (±0.1)	0.336 (±0.002)	156.2 (±7)	0.3[a]	146.2 (±0.2)	0.340 (±0.01)	80.9	0.401
650	176.9 (±0.1)	0.337 (±0.002)	155.0 (±1.1)	0.372 (±0.022)	146.4 (±0.5)	0.343 (±0.005)	127.4	0.411
850	173.6 (±0.1)	0.334 (±0.001)	160.1 (±1.1)	0.340 (±0.006)	148.9 (±0.1)	0.308 (±0.001)	161.9	0.355

[a] Poisson's ratio of 6ScSZ at 450 °C was estimated due to the non-applicability of the IET-method at that temperature.

Table 2
Median strength for varying temperature and the corresponding fracture toughness calculated according to Equation (3) from high temperature strength data.

Temperature (°C)	3YSZ		6ScSZ		6Sc1CeSZ		10Sc1CeSZ	
	$\sigma_{50\%}$ (MPa)	K_{Ic} (MPa m$^{1/2}$)	$\sigma_{50\%}$ (MPa)	K_{Ic} (MPa m$^{1/2}$)	$\sigma_{50\%}$ (MPa)	K_{Ic} (MPa m$^{1/2}$)	$\sigma_{50\%}$ (MPa)	K_{Ic} (MPa m$^{1/2}$)
25	1595	5.0[a] (±0.24)	1360	4.1[b] (±0.25)	1929	3.7[b] (±0.1)	665	1.8[b] (±0.17)
250	1548	4.8	1365	4.1	1872	3.6	668	1.8
350	–	–	–	–	–	–	504	1.4
450	1107	3.5	973	2.9	1374	2.6	364	1.0
650	831	2.6	691	2.1	939	1.8	397	1.1
850	685	2.1	499	1.6	756	1.4	463	1.3
950	–	1.9[a] (±0.21)	–	–	–	–	–	–

[a] Values taken from Ref. [24].
[b] Values taken from Ref. [13].

to thermal mismatch strains and local stresses due to an uneven clamping of the cell [27]. Since clamping loads can become significant in magnitude and are present from RT to operating temperature, the temperature behaviour of the biaxial fracture strain ($\varepsilon_{frac,biax} = \sigma_{frac,biax}(1-\nu)/E$) is considered as well and shown in Fig. 3. For 6ScSZ and 6Sc1CeSZ the RT level is maintained until $T = 450$ °C, from where it then drops down to 50% at 850 °C. 3YSZ behaves similarly but begins its decay already at $T = 250$ °C. Again

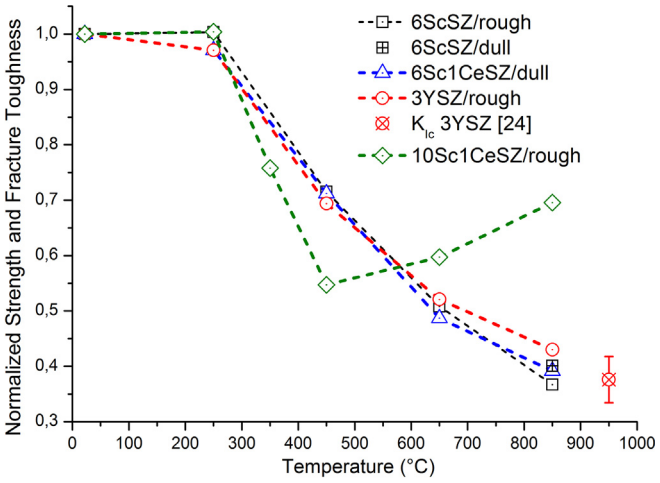

Fig. 2. Temperature dependent fracture toughness normalised to room temperature values, including the normalised toughness of 3YSZ at 950 °C taken from Ref. [24].

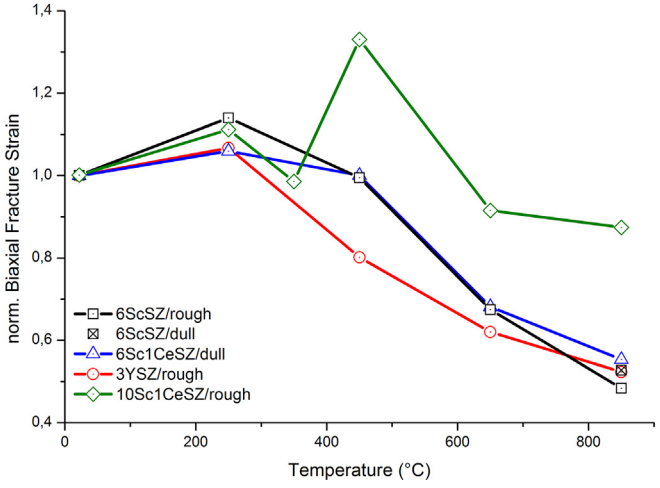

Fig. 3. Biaxial fracture strain normalised to the RT values for different zirconia compounds and varying temperature.

10Sc1CeSZ shows a complete different trend. Its strength minimum at 450 °C is overcompensated by the Young's modulus and turns into a maximum, while it retains at 850 °C 90% of its RT fracture strain.

3.3. Strength at high temperature affected by sub critical crack growth

If strength determining flaws are accessible by moisture which is omnipresent in environmental air, these flaws tend to grow subcritically if a stress below the respective fracture stress is applied. Thus the strength itself becomes dependent on the time under load, which leads to a limited lifetime. Since the perspective operating time of a fuel cell can be up to eight years including several thermo cycles, while being subjected to humid environments on both sides, this effect has to be measured for varying temperatures. Typically SCCG is described via the crack growth rate da/dt of a crack or a flaw with the size a, which typically follows a Paris law in the form of:

$$\frac{da}{dt} = v_0 \left(\frac{K_{app}}{K_{Ic}}\right)^n \tag{5}$$

where v_0 is the reference velocity, which is the crack growth rate when the applied stress intensity factor K_{app} reaches the fracture toughness K_{Ic}. n is the so called crack growth exponent, which is lower the more sensitive a material is to moisture. Since K_{app} depends not just on the applied stress σ_{app} but also on the crack size a, expressed by the Griffith criterion:

$$K_{app} = \sigma_{app} Y \sqrt{\pi a} \tag{6}$$

with Y being the geometry factor of the crack, which was set to $Y = 0.85$ to reflect semi-elliptical surface cracks [28], which remains independent of the crack size for small cracks. This phenomenon can now be described by the two parameters v_0 and n, which have to be determined for a defined temperature and humidity. By inserting Equation (6) in Equation (5) a differential equation is obtained. If the applied stress is constantly increased with the load rate $\dot{\sigma}$, following expression can be derived [1]:

$$\log \sigma_{app}\left(t_f\right) = \log \sigma_f = \frac{1}{n+1}\log \dot{\sigma} + \frac{1}{n+1}\log\left(\frac{2K_{Ic}^2\left(n+1\right)}{v_0 \pi Y^2 \left(n-2\right)}\sigma_{inert}^{(n-2)}\right) \tag{7}$$

with σ_{inert} being the inert strength in the absence of the SCCG effect and σ_f the fracture stress. By measuring the strength as a function of the load rate, it is possible to determine the crack growth

parameters. For the four zirconia compounds investigated in the present study these parameters have been already published at RT for different humidity levels by Fleischhauer et al. [13]. It was found that already at RT the strength is affected drastically by SCCG even in small time scales. In the present study, 6ScSZ has been chosen to investigate how this effect changes with temperature by measuring the strength as a function of the load rate while keeping the absolute humidity constant at a partial pressure of $p_{H_2O} = 11.5$ mbar (43% relative humidity at $T = 22$ °C) and applying the same data analysis procedure as in Ref. [13]. The constant humidity was ensured by bubbling a dry argon (80%)/oxygen (20%) mixture through a saturated aquatic K_2CO_3-solution kept at $T = 22$ °C and is supposed to represent environmental air. The results including the data at RT taken from Ref. [13] are shown in Fig. 4.

At $T = 250$ °C the strength shifts to greater values, which leads to a strengthening of 6ScSZ at elevated temperatures, while being subjected to humid environments. This phenomenon has not been reported before in literature and is at this point not soundly understood. Interestingly this effect apparently requires a certain time under load, as no strength increase has been found for the samples tested at a very high load rate of 1 GPa s^{-1}, although they were held equally long compared to the other samples at 250 °C prior to the test. It is also remarkable that the crack growth exponent just significantly changes at $T = 450$ °C towards a much lower value. At $T = 650$ °C instead of a continuous strength decay a formation of a threshold strength σ_{th} is recognisable, which at $T = 850$ °C is even at the level of the inert strength. For the rough side of 3YSZ the threshold strength at $T = 650$ °C and a partial water vapour pressure of $p_{H_2O} = 8$ mbar (30% relative humidity at $T = 22$ °C) has been determined to be $\sigma_{th,650\ °C} = 797$ MPa ($\sigma_{inert,650\ °C} = 840$ MPa), while at 850 °C no significant crack growth occurred as well.

Hence the effect of SCCG becomes very limited at higher and for the operation of SOFCs rather relevant temperatures. This trend has been already reported for 3YSZ, 8YSZ and also for magnesia partially stabilized zirconia by Alcala and Anglada [5], Choi [29] and Davidson et al. [30], respectively and leads to the general assumption for zirconia compounds that at temperatures greater than 800 °C no significant humidity related SCCG occurs.

4. Discussion

Having determined the strength distribution, the temperature dependence and the SCCG parameter, it is finally possible to compare and assess the investigated zirconia compounds regarding their strength in humid environments for different temperatures. If no SCCG occurs the strength σ is a function of the required failure probability and the loaded surface area and can be described via the standard Weibull distribution [1]:

$$\sigma(S,P,T) = \left(\frac{S_0}{S}\sigma_0(T)^m \ln\left(\frac{1}{1-P}\right)\right)^{\frac{1}{m}} \tag{8}$$

where the temperature dependency is expressed through the characteristic strength σ_0, which can be obtained from RT values by applying Equation (3). If SCCG has to be taken into account, the respective time dependent strength is obtained by the combination of Equations (5–6) and (8) and becomes:

$$\sigma_{stat}(T,S,P,t_f) = \left(\frac{K_{Ic}^2\left(\frac{S_{eff}}{S}\sigma_0(T)^m ln\left(\frac{1}{1-P}\right)\right)^{\frac{n(T)-2}{m}}}{v_0(T)t_f\pi Y^2\left(\frac{n(T)}{2}-1\right)}\right)^{1/n(T)} \tag{9}$$

with the reference velocity v_0 and the crack growth exponent n being temperature dependent as well. If SCCG reaches a threshold, Equation (8) is applied again inserting the respective time independent threshold strength instead of the inert strength. Taking the strength data of the dull sides (side of the cast tape which was opposite to the support foil) of commercial 3YSZ, 6ScSZ and 10Sc1CeSZ tapes from a previous study [13], given in Table 3, the influence of temperature and SCCG can be quantitatively assessed for a given system and its respective load environment. To give an example how these different dependencies influence the strength, the load environment of the μ-CHP (small scale combined heat and power plant) Galileo 1000 N of Hexis AG (Winterthur, Switzerland) [31] is considered for further discussion, which has been described in a previous study [27]. At $T = 850$ °C it is assumed that the peak loads are caused by thermal stresses, which effectively load a surface area S of approximately 10 cm^2 of the total cell area of 200 cm^2. For simplicity the same area is kept constant for varying temperatures. As one single failed cell might harm a whole stack and can lead to significant performance losses, a required failure probability P of 1:10,000 is assumed, which means that in average, roughly every hundredth stack might contain a failed cell. The prospective operating time of the stack is 8 years, of which the system remains idle between 0 and 50% of the time, depending on the heat demand. Therefore, a lifetime t_f of four years is considered for RT, while at $T = 850$ °C no time dependent strength decay is expected. According to Equations (8) and (9) the respective strength of the three zirconia compounds is shown in Fig. 5 including the 90% confidence intervals.

Apart from the thermal stresses, residual stresses and clamping loads are also present at all times, thus also during thermo cycling. Hence the strength of 6ScSZ is plotted also for 250 and 450 °C according to Equation (9) assuming a lifetime of twenty days, which is a rough and conservative estimation of the cumulated time the electrolyte is subjected to SCCG at the respective temperature during cooling down and heating up, as one complete thermo cycle requires one day, assuming twenty cycles during 8 years. At 650 °C the threshold strength observed for 3YSZ and 6ScSZ is translated analogue to Equation (4) into a threshold stress intensity factor $K_{I,th}$, below which no SCCG occurs, applying the respective inert strength and the corresponding fracture toughness at 650 °C. Again following Equation (4) the RT strength given in Table 3 can be translated into the SCCG affected strength at 650 °C applying the threshold $K_{I,th}$ instead of the fracture toughness. The strength of 3YSZ at 450 °C is given, using the $K_{I,th} = 2.2$ MPa $m^{½}$ at 450 °C given

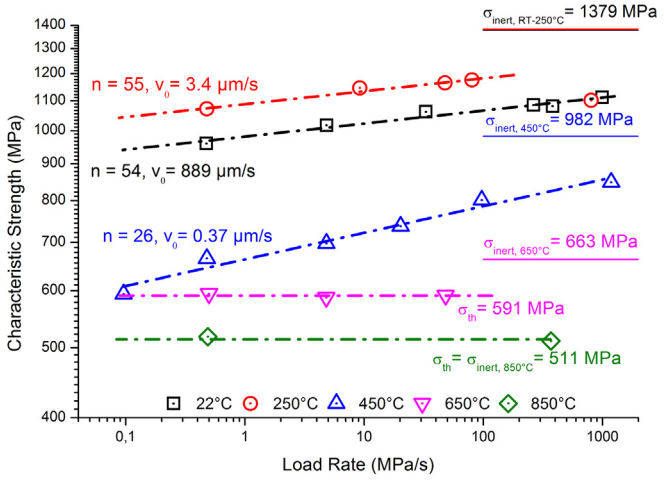

Fig. 4. Strength dependence on the load rate of 6ScSZ at varying temperatures including the respective inert strength levels, SCCG parameter and observed threshold strength at $T = 650$ °C and $T = 850$ °C. The inert strength is determined at a loading rate close to 1 GPa s^{-1}.

Table 3
Selection of strength and SCCG data at RT used for further discussion taken for 8YSZ from Ref. [32] and the other compounds from Ref. [13]. The values given in the brackets are the 90% confidence intervals.

	Characteristic strength σ_0 (MPa)	Weibull modulus m	Reference surface area S_0 (mm^2)	Crack growth exponent n	Reference velocity v_0 (m s^{-1})
3YSZ	1433 (1501|1369)	10 (15|7.2)	15	55	0.09
6ScSZ	1126 (1153|1100)	11 (13.6|9.2)	18	54	0.9
10Sc1CeSZ	1136 (1168|1106)	12 (15.0|9.2)	0.025	37	0.004
8YSZ	446[a] (468|425)	6.7 (8.4|5.2)	9[b]	–	–
8YSZ (900 °C)	282 (296|268)	8 (10.7|5.7)	9[b]	–	–

[a] Taken as inert strength, although measured in humid air.
[b] Values roughly estimated, as they are not explicitly given.

by Ref. [5], while the respective strength of 8YSZ at RT and 900 °C is given as comparison and taken from Ref. [32]. Among all the published data, this data shows until now the highest achievable strength at high temperatures for this compound and is at the same time the most dependable since it was obtained testing 30 and 20 specimens, respectively applying a low friction high temperature RoR set up, which ensured a high level of accuracy. The RT SCCG affected strength was calculated, using the threshold stress intensity factor $K_{I,th} = 0.72$ MPa m^{½} and the fracture toughness of $K_{Ic} = 1.51$ MPa m^{½}.

When taking SCCG into account the strength over the temperature of 3YSZ and 6ScSZ does not show a monotonic decay as for the inert strength depicted in Fig. 2. At $T = 450$ °C the strength becomes comparable with that at $T = 850$ °C, while it rises again when coming to lower temperatures. Considering 10Sc1CeSZ, it is revealed, that SCCG leads to a lower strength at RT than at 850 °C, where it surprisingly even reaches up to the levels of the tetragonal zirconia compounds. 8YSZ on the other hand appears to be the weakest of the common zirconia. Comparing the strength to the magnitude of thermal stresses which are expected to rise due a generally given inhomogeneous temperature distribution throughout the cell and which are typically in the range of 50–60 MPa [16,27,33,34], it is revealed that 8YSZ is not suited for the application in electrolyte supported fuel cells.

To evaluate the risk of cell failure the strength, which can be interpreted as a design stress, is plotted for 6ScSZ, 10Sc1CeSZ and 3YSZ at RT, assuming again four years of lifetime and at 850 °C versus the failure probability for varying loaded surface areas, as shown in Fig. 6. Assuming again thermal stresses in the range of 50–60 MPa the depicted zirconia compounds show a high reliability even with loading surface areas as large as 100 cm^2. Interestingly the differences between the three materials at 850 °C are small if not negligible considering the confidence intervals given in Fig. 5. Next to thermal stresses the electrolyte is also subjected to stresses due to the clamping, as the contact between the metallic interconnect (MIC) and the cell is never perfectly flat and leads to local bending, and residual stresses due to thermal mismatch of the cell components. The residual stresses are small at operating temperatures, while they increase if the cell is cooled down to RT, putting the electrolyte under a slight compressive load (~20 MPa) [27,35]. Hence the residual stresses can be neglected for further discussion. Stresses due to clamping on the other hand can become significant and might lead to local damage [27]. Fig. 6 can now be used to reveal the allowed magnitude of clamping stresses. For 3YSZ and 6ScSZ the respective analysis just has to be made at operating temperatures, since the strength at RT is significantly higher. Depending on the tolerated risk of failure and the area where the peak stresses (superposition of all expected loads) act on, stresses apart from thermal stresses (assumed to be ~50 MPa) can reach between 50 and 150 MPa. For 10Sc1CeSZ the difference in strength between RT and 850 °C is roughly the amount for the reported thermal stresses, hence the allowed clamping loads for this material have to be oriented on the RT strength level, which results in a similar range of 50–150 MPa as for the tetragonal compounds. Hence according to the strength data given in Table 3, the highly conductive 10Sc1CeSZ compound can be regarded as

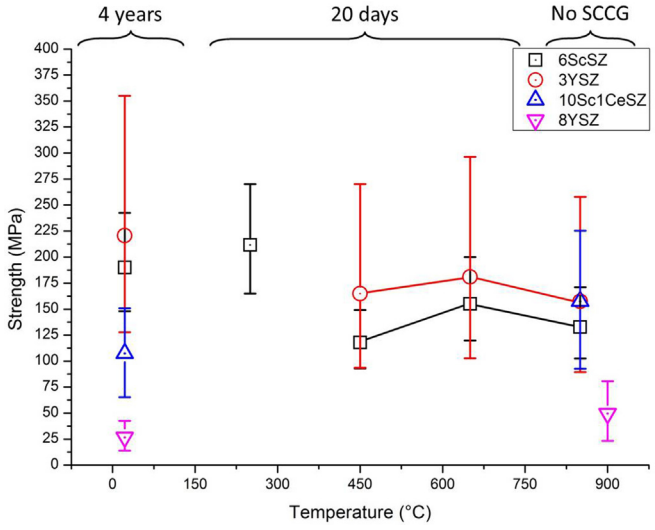

Fig. 5. Strength of different zirconia tapes including the 90% confidence intervals at varying temperatures for $S = 10$ cm^2 and $P = 0.0001$, taking SCCG for different lifetimes into account.

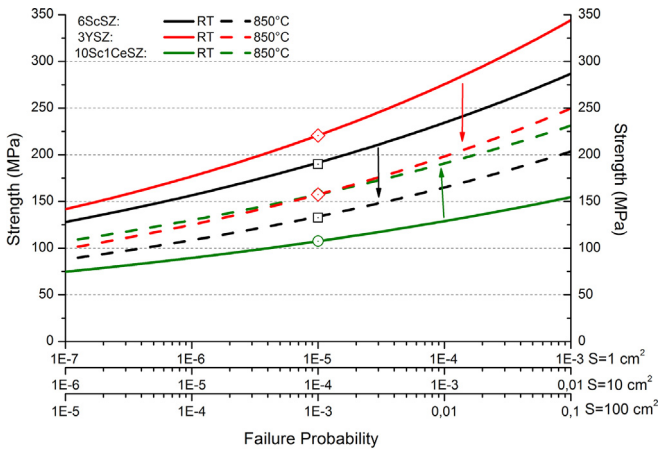

Fig. 6. Strength of 10Sc1CeSZ, 3YSZ and 6ScSZ versus failure probability for different considered loaded surface areas at RT and 850 °C. Also plotted are the respective points given in Fig. 5.

competitive compared to 3YSZ and 6ScSZ from a reliability perspective.

5. Conclusion

(i) The change of strength of the tested zirconia compounds with temperature can be attributed solely to the change of the fracture toughness, so that any given RT strength can be translated into the respective strength at elevated temperatures.
(ii) The tetragonal zirconia compounds have similar monotonic temperature decay of their inert strength, while the cubic 10Sc1CeSZ shows a minimum at 450 °C. The minimum of the inert fracture strain lies for all compounds at 850 °C.
(iii) At 850 °C SCCG does not affect the strength of these zirconia compounds, while 6ScSZ shows the greatest sensitivity at 450 °C. Taking SCCG into account, the temperature behaviour of the strength becomes more complex and depends basically on the required lifetime of the component at each temperature it is exposed to. This also highlights the importance of the determination of the inert strength, as it is crucial to calculate the strength degradation and correspondingly the lifetime.
(iv) Based on the requirements associated with the operating conditions of the Galileo 1000 N, it was found that it is sufficient to assess the reliability of the tetragonal zirconia compounds just at the operating temperature, whereas for 10Sc1CeSZ at least the stress environment at RT has to be considered as well, since its fracture strain and stress was found to be lower at RT than at 850 °C.
(v) Based on the strength data of a previous study, the overall stress levels that the electrolyte experiences while maintaining a level of reliability has to be limited between 100 and 200 MPa, depending on the specifics of the respective system, which appears feasible. It was further found that 10Sc1CeSZ can be regarded as competitive compared to 6ScSZ and 3YSZ.
(vi) The Ball-on-3-Balls bending test proves to be very suitable to characterise material specific properties such as the change of strength with temperature or the determination of the sub critical crack growth parameter, as it is very accurate and requires only small samples with a rectangular shape. Additionally any gaseous media can easily be applied during testing, to ensure a defined environment.

Acknowledgements

The authors would like to thank R. Bächtold and U. Weissen for the unconditional support. Furthermore, the funding of this work by the Swiss Federal Office of Energy under the contract no. 8100076; SI/500084-02 and by Swisselectric Research within the SOF–CH-ESC project is gratefully acknowledged.

References

[1] R. Danzer, T. Lube, P. Supancic, R. Damani, Adv. Eng. Mater. 10 (2008) 275–298.
[2] M. Radovic, E. Lara-Curzio, G. Nelson, Ceram. Eng. Sci. Proc. 27 (2007) 373–381.
[3] W.M. Rainforth, F.L. Lowrie, R.D. Rawlings, J. Eur. Ceram. Soc. 20 (2000).
[4] A.N. Kumar, B.F. Sorensen, Mater. Sci. Eng. A333 (2002) 380.
[5] J. Alcala, M. Anglada, Mater. Sci. Eng. A 232 (1997) 103–109.
[6] A. Selcuk, A. Merere, A. Atkinson, J. Mater. Sci. 36 (2001) 1173–1182.
[7] B.F. Sorensen, S. Primdahl, J. Mater. Sci. 33 (1998) 5291–5300.
[8] J. Malzbender, P. Batfalsky, R. Vaßen, V. Shemet, F. Tietz, J. Power Sources 201 (2012) 196–203.
[9] J. Chevalier, L. Gremillard, A.V. Virkar, D.R. Clarke, J. Am. Ceram. Soc. 92 (2009) 1901–1920.
[10] M. Chen, Y.L. Liu, A. Hagen, P.V. Hendriksen, F.W. Poulsen, Fuel Cells 9 (2009) 833–840.
[11] A. Nakajo, J. Kuebler, A. Faes, U.F. Vogt, H.J. Schindler, L.-K. Chiang, S. Modena, J. Van Herle, T. Hocker, Ceram. Int. 38 (2012) 3907–3927.
[12] Y. Chen, A. Aman, M. Lugovy, N. Orlovskaya, S. Wang, X. Huang, T. Graule, J. Kuebler, Fuel Cells 13 (2013) 1068–1075.
[13] F. Fleischhauer, M. Terner, R. Bermejo, R. Danzer, T. Graule, A. Mai, J. Kuebler, J. Power Sources (2014) (submitted, POWER-D-14-02559R1).
[14] J. Malzbender, R.W. Steinbrech, J. Eur. Ceram. Soc. 27 (2007) 2597–2603.
[15] R. Clague, A.J. Marquis, N.P. Brandon, J. Power Sources 221 (2013) 290–299.
[16] A. Nakajo, Z. Wuillemin, J. Van herle, D. Favrat, J. Power Sources 193 (2009) 203–215.
[17] S.P.S. Badwal, F.T. Ciacchi, D. Milosevic, Solid State Ionics 136–137 (2000) 91–99.
[18] N. Orlovskaya, S. Lukich, G. Subhash, T. Graule, J. Kuebler, J. Power Sources 195 (2010) 2774–2781.
[19] S. Spinner, W.E. Tefft, Proc. ASTM 61 (1961).
[20] R. Danzer, P. Supancic, W. Harrer, J. Ceram. Soc. Jpn. 114 (2006) 1054–1060.
[21] A. Börger, P. Supancic, R. Danzer, J. Eur. Ceram. Soc. 22 (2002) 1425–1436.
[22] S. Giraud, J. Canel, J. Eur. Ceram. Soc. 28 (2008) 77–83.
[23] T. Kushi, K. Sato, A. Unemoto, S. Hashimoto, K. Amezawa, T. Kawada, J. Power Sources 196 (2011) 7989–7993.
[24] J. Kuebler, U.F. Vogt, D. Haberstock, J. Sfeir, A. Mai, T. Hocker, M. Roos, U. Harnisch, Fuel Cells 10 (2010) 1066–1073.
[25] M. Matsui, T. Soma, I. Oda, J. Am. Ceram. Soc. 59 (1986) 198–202.
[26] J.J. Mecholsky Jr., Mater. Lett. 60 (2006) 2485–2488.
[27] F. Fleischhauer, A. Tiefenauer, T. Graule, R. Danzer, A. Mai, J. Kuebler, J. Power Sources 258 (2014) 382–390.
[28] S. Strobl, P. Supancic, T. Lube, R. Danzer, J. Eur. Ceram. Soc. 32 (2012) 1491–1501.
[29] S.R. Choi, in: D. Bray (Ed.), 22nd Annual Conference on Composites, Advanced Ceramics, Materials, and Structures: B, Amer Ceramic Soc, Westerville, 1998, pp. 293–301.
[30] D.L. Davidson, J.B. Campbell, J. Lankford, Acta Metall. Mater. 39 (1991) 1319–1330.
[31] A. Mai, B. Iwanschitz, U. Weissen, R. Denzler, D. Haberstock, V. Nerlich, A. Schuler, in: S.C. Singhal, K. Eguchi (Eds.), ECS Transactions, 2011, pp. 87–95.
[32] A. Atkinson, A. Selcuk, Solid State Ionics 134 (2000) 59–66.
[33] A. Nakajo, Z. Wuillemin, J. Van herle, D. Favrat, J. Power Sources 193 (2009) 216–226.
[34] H. Severson, M. Assadi, J. Fuel Cell Sci. Technol. 10 (2013).
[35] J. Laurencin, G. Delette, F. Lefebvre-Joud, A. Dupeux, J. Eur. Ceram. Soc. 28 (2008) 1857–1869.